2013 American Control Conference (ACC)
Washington, DC, USA, June 17-19, 2013

Adaptive Circadian Argument Estimator and Its Application to Circadian Argument Control

Jiaxiang Zhang, John T. Wen, Agung Julius
Department of Electrical, Computer, & Systems Engineering, Rensselaer Polytechnic Institute, Troy, NY 12180
{zhangj16,wenj,juliua2}@rpi.edu

Abstract— **Disruption of the circadian rhythm is detrimental to human well being, with consequences ranging from lower productivity, sleep disorder, to more serious health problems. Accurate estimation of circadian argument is critical to the assessment and treatment of circadian disruption. Circadian argument estimate is also essential for light-based circadian entrainment. Direct measurements of circadian rhythm markers such as dim light melatonin onset are inconvenient and acquired at best at low rate. Wearable continuous measurement such as actigraph is convenient but is masked by many other factors. In this paper, we present a new circadian rhythm estimation scheme based on a type of frequency tracker, called adaptive notch filter (ANF) which is commonly used in signal processing. ANF is designed to track the gain and phase of a single sinusoid from noisy data. We extend the classic ANF to multiple harmonics needed in circadian rhythm tracking. The local stability and high order harmonics robustness are analyzed. The highly noisy indirect measurements result in unreliable amplitude estimate, but the phase estimate is generally quite robust. We use this phase estimate combined with the light input to construct a black-box linear time varying (LPV) system description, parameterized by the phase estimate. The LPV model predicts the circadian rhythm response to light inputs and can be used for the design of light-based feedback control. The proposed modeling and control method is applied to three different models of circadian rhythm: Kronauer's human circadian model, Leloup's *Drosophila* circadian model and *Neurospora* circadian model. Simulation shows that our approach can generate reliable circadian argument estimation and effective gain-scheduled control of the circadian rhythm without any knowledge of the underlying model. The ability to generate circadian estimate, model, and control based only on input/output data opens up the tantalizing possibility of personalized circadian rhythm estimator and light therapy.**

I. Introduction

Disruption of the synchrony between the solar day and human internal master clock that regulates and generates circadian rhythms has been linked to a variety of maladies. Circadian disruption, as experienced by night shift workers or by those traveling multiple time zones can lead to low productivity, digestive problems and decreased sleep effectiveness. Long term effects of circadian disruption have been linked to serious health problems, such as increased risk of cancer, cardiovascular disease, diabetes and obesity.

Various groups have proposed the use of light to entrain the circadian rhythm [1]–[8]. Circadian regulation using chemical intervention (e.g., melatonin, modafinil) has also been studied [9]–[11]. Most of the work on light-based circadian rhythm regulation is open loop in nature, based on the response curve (PRC), the amount of the steady state phase shift due to a specified light pulse input at different circadian phase [9], [12]. Optimal control has only been recently considered [8], [13], [14]. There are also commercial products for self-administered light therapy to address seasonal affective disorder [15], [16]. They are low cost and convenient, but only provide rough guideline on their usage for circadian rhythm regulation. Feedback control of the light therapy is attractive as it could accommodate variations between individuals and disturbances from the environment. Some closed loop strategies have been suggested and demonstrated in simulation [7], [17], but a reasonable estimation of the circadian argument based on physiological sensor measurements is needed for deployment.

The circadian rhythm may be assessed by measuring the circadian data. For humans, certain hormones related to circadian rhythm such as melatonin, cortisol, alpha amyloid, have also been used as circadian data. These types of direct measurements are intrusive in terms of collection (blood serum, saliva), time consuming and expensive in terms of analysis. As a result, the sampling rate is very low, at best once per several hours, over a limited duration in experimental trials. More common types of circadian data are the use of indirect markers, such as body temperature, heart/pulse rate, activity level, etc. Locomotor activity, in particular, together with tools such as actogram (or actigraph), has long been used in Drosophila, rodent, and human studies [18]–[23].

Numerous techniques for circadian data analysis have been proposed (see review in [24]). Most are batch in nature, meaning that the circadian argument is extracted in postprocessing of a batch of circadian data. These techniques include manual inspection of actogram [25], statistical method [26], Fourier analysis [24], cosinor [27], and activity onset [28]. A number of recursive methods, where circadian rhythm estimate is updated with new measurements, have also been proposed. There are two classes of algorithms, depending on if an underlying input/output model is assumed. Extended Kalman Filter (EKF) [29] and Particle Filter [30] are model-based method using the empirical nonlinear oscillator model (relating input light intensity to the output core body temperature). Gliding cosinor is a model-free approach which works the same as cosinor but for a fixed window of the past data [31].

978-1-4799-0178-4/$31.00 ©2013 AACC

In this paper, we present a model-free circadian argument estimation scheme by using a type of frequency tracker, called adaptive notch filter (ANF). Based on the filter proposed in [32], we modify the ANF to accommodate the non-zero mean and non-sinusoidal waveform of the circadian data. We establish the local stability and robustness properties of the extended ANF algorithm. The effectiveness of ANF on *Drosophila* and rat locomotor activity data is demonstrated in [33].

Using the light pulse applied at different circadian arguments as input and the estimated circadian arguments using ANF as output, we identify a family of linear time invariant (LTI) systems to model the cascaded system of the circadian response and the ANF. This family of LTI models, parameterized by the circadian argument, form a linear parameter varying (LPV) system. The LPV description allows prediction of the circadian response under different lighting conditions. The LPV system may also be used to construct a corresponding family of LTI feedback light control based on the ANF output feedback. Such gain scheduled control allows effective entrainment of the estimated circadian argument to the desired profile.

To generate test data and evaluate the performance of the proposed method, we use three accepted circadian models in the literature, including an empirical model for human circadian response to light input proposed by Kronauer [34], and biochemical models for *Drosophila* and *Neurospora* [35].

II. Circadian Argument Estimation

The circadian data is approximately a periodic signal. Its waveform varies with the species, individuals in the species, types of physiological measurement, and environment condition. We assume the signal may be represented by a finite Fourier series, and the circadian argument is represented by the argument of the fundamental harmonic. As a reliable model, whether mechanistic or phenomenological, is almost never available for circadian rhythm, estimation of the circadian phase based on direct extraction of the harmonics from measurements is a reasonable and robust approach. Assume the following form of the circadian signal y:

$$y(t) = \sum_{k=1}^{N} a_k \sin(k\omega^* t + \phi_k) + d + w(t)$$

where d is a constant bias, w is a zero-mean white noise. Define the arguments of the harmonics as

$$\theta_k(t) = k\omega^* t + \phi_k,\ k \in \{1,\ldots,N\}. \tag{1}$$

We will work with $\theta_1(t)$ directly in terms of estimation and control since it is difficult to reliably estimate time varying ω and $\phi_1(t)$ (e.g., under varying light input) separately. There are several algorithms for adaptive frequency estimation [36] with relative performance trade-offs in terms of the rate of convergence, domain of convergence, and robustness with respect to noise and distortion, etc. We will focus on the ANF approach in this paper because of its stability property and superior convergence property under good initial guess of the period (roughly 24 hours). The original ANF proposed in [32] can only track a single sinusoid with zero mean. To address more general waveforms, we modify the ANF by adding a constant bias and higher order harmonics. We will present below local stability and robustness analysis of the ANF with second order harmonics. Similar stability and robustness results may be obtained for higher order harmonics. The proposed second order ANF is given by:

$$\dot{x} = A(\omega)x + B(\omega)y, \tag{2}$$

$$\dot{\omega} = \gamma_\omega f(y,\omega,x). \tag{3}$$

with

$$A(\omega) = \begin{pmatrix} 0 & 1 & 0 & 0 & 0 \\ -\omega^2 & -2\zeta\omega & 0 & -\zeta\omega & -\omega^2 \\ 0 & 0 & 0 & 1 & 0 \\ 0 & -8\zeta\omega & -4\omega^2 & -4\zeta\omega & -4\omega^2 \\ 0 & -\frac{2\zeta\gamma_d}{\omega} & 0 & -\frac{\zeta\gamma_d}{\omega} & -\gamma_d \end{pmatrix},$$

$$B(\omega) = [0,\omega^2,0,(2\omega)^2,\gamma_d]^T,$$

$$f(y,\omega,x) = -x_1\omega^2(y - x_5 - \frac{2\zeta x_2}{\omega} - \frac{2\zeta x_4}{2\omega})$$

$$\hat{y} = x_5 + \frac{2\zeta x_2}{\omega} + \frac{2\zeta x_4}{2\omega}$$

where $x \in \mathbb{R}^5$, ω and x_5 are the estimated frequency of the fundamental harmonic and the constant bias, respectively; y is the circadian data; the filtered circadian data $\hat{y}$ is the output of ANF; γ_ω and γ_d are the adaptation rate, and ζ is a tunable parameter of the filter. γ_ω, γ_d and ζ are all positive.

Theorem 1: For the system defined by (2) and (3) with input $y(t) = \sum_{k=1}^{2} a_k sin(k\omega^* t + \phi_k) + d$, the parameter adaptation (3) has a stable equilibrium at

$$\omega = \omega^*, \tag{4}$$

and the steady state response of (2) is

$$x_1 = -\frac{a_1\cos(\omega^* t + \phi_1)}{2\zeta},\ x_2 = \frac{a_1\omega^*\sin(\omega^* t + \phi_1)}{2\zeta}, \tag{5}$$

$$x_3 = -\frac{a_2\cos(2\omega^* t + \phi_2)}{2\zeta},\ x_4 = \frac{a_2\omega^*\sin(2\omega^* t + \phi_2)}{\zeta},\ x_5 = d. \tag{6}$$

Proof: In order to use the integral manifold of slow adaptation [37] to show the local stability of (2)-(3) with periodic input y, the adapted constant bias x_5 is considered as a state variable. With a frozen parameter ω, the dynamics of (2) is LTI system. Defining

$$H(\omega_1,\omega_2) = (i\omega_1 I - A(\omega_2))^{-1}B(\omega_2), \tag{7}$$

we can verify that the steady state response of the LTI system (2) is

$$x^0(t,\omega,\omega^*) = \sum_{k=1}^{2}[a_k\Re(H(k\omega^*,\omega))\sin(k\omega^* t + \phi_k) + a_k\Im(H(k\omega^*,\omega))\cos(k\omega^* t + \phi_k)] + [0,0,0,0,d]^T.$$

If the state vector x is deviated from x^0, we introduce the deviation of x from x^0 as a new state variable

$$\tilde{x} = x - x^0$$

and the ANF can be rewritten as

$$\dot{\tilde{x}} = A(\omega)\tilde{x} - \frac{\partial x^0(t,\omega)}{\partial \omega}\gamma_\omega f(y,\omega,x^0+\tilde{x}), \dot{\omega} = \gamma_\omega f(y,\omega,x^0+\tilde{x}) \tag{8}$$

The existence of the integral manifold for (8) can be shown by using Theorem 3.1 in [37], and the three assumptions of the theorem are all satisfied:

1) $A(\omega)$ is exponentially stable.
2) $x^0(t,\omega,\omega^*)$ and $\frac{\partial x^0(t,\omega,\omega^*)}{\partial \omega}$ are bounded and the latter is Lipschitz in ω.
3) $f(y,\omega,x^0+\tilde{x})$ is continuous and Lipschitz in ω and y.

Assuming the deviation $\tilde{x}$ is small, the update law can be approximated by

$$\dot{\omega} = \gamma_\omega f(y(t),\omega,x^0(t,\omega,\omega^*)). \tag{9}$$

For $N=2$, it can be verified that the $\omega = \omega^*$ is an equilibrium of (9). Defining $\delta\omega$ as the deviation of ω from ω^*, we linearize (9) at $\omega = \omega^*$:

$$\delta\dot{\omega} = \alpha(t)\delta\omega. \tag{10}$$

where $\alpha(t) = \gamma_\omega(\frac{\partial f}{\partial \omega} + \frac{\partial f}{\partial x^0}\frac{\partial x^0(t,\omega,\omega^*)}{\partial \omega})|_{\omega=\omega^*}$. Because $y(t)$ and $x^0(t,\omega,\omega^*)$ are both periodic with period $T = \frac{2\pi}{\omega^*}$, $a(t)$ is also periodic. It can be verified that

$$\int_t^{t+T} \alpha(s)ds = -\gamma_\omega T\frac{a_1^2}{\omega^*\zeta^2} < 0$$

The solution of (10) is $\delta\omega(t) = \delta\omega(t_0)e^{\int_{t_0}^t \alpha(s)ds}$. As $t\to\infty$,

$$\lim_{t\to\infty}\int_{t_0}^t \alpha(s)ds = \lim_{t\to\infty}\left(-\sum_{n=1}^{\lfloor\frac{t-t_0}{T}\rfloor}\gamma_\omega T\frac{(a_1^*)^2}{\omega^*\zeta^2} + O\right) = -\infty.$$

where $O = \int_{t-T\lfloor\frac{t-t_0}{T}\rfloor}^t \alpha(s)ds$ is bounded. So $\delta\omega(t)\to 0$ as $t\to\infty$, and the parameter ω converges to ω^*. The steady state response $x^0(t,\omega^*,\omega^*)$ can be verified to be (5) - (6). ■

Remark 1: Using the same procedure, it can be shown that for ANF with third order harmonics and input $y(t) = \sum_{k=1}^3 a_k sin(k\omega^* t + \phi_k(t)) + d$, (4) - (6) and the local stability results still hold.

Remark 2: According to (5), we proposed the circadian argument estimate as

$$\hat{\theta} = -\tan^{-1}\left(\frac{x_2}{\omega x_1}\right) \tag{11}$$

Circadian data may have higher order harmonics, so we further analyze the local stability of the proposed ANF under higher order harmonics:

Theorem 2: For the system defined by (2) and (3) with input $y(t) = \sum_{k=1}^N a_k sin(k\omega^* t + \phi_k) + d$, if there exists ω_a^* such that the following are satisfied:

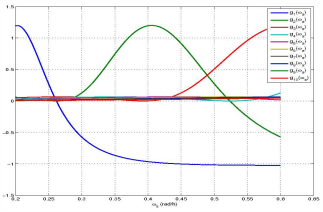

Fig. 1. $g_k(\omega_a), k\in\{1,\dots 10\}$ for $\zeta = 0.3$, $\omega^* = \frac{2\pi}{24}$(rad/h) and $\gamma_d = 0.001$.

$$\sum_{k=1}^N a_k^2 g_k(\omega_a^*) = 0, \tag{12}$$

$$\frac{\partial\sum_{k=1}^N a_k^2 g_k(\omega_a)}{\partial\omega_a}|_{\omega_a=\omega_a^*} < 0, \tag{13}$$

where

$$g_k(\omega_a) \triangleq -R_{1k}\left(1 - \frac{2\zeta}{\omega_a}R_{2k} - \frac{\zeta}{\omega_a}R_{4k} - R_{5k}\right) - I_{1k}\left(-\frac{2\zeta}{\omega_a}I_{2k} - \frac{\zeta}{\omega_a}I_{4k} - I_{5k}\right);$$

R_{mk} and I_{mk} are the real part and imaginary part of the m^{th} element of $H(k\omega^*,\omega_a)$ defined by (7), there exists a $\gamma_{\omega a}$ such that when $0<\gamma_\omega<\gamma_{\omega a}$, (2)-(3) is locally stable at

$$\omega = \omega_a^*,$$

$$x(t) = \sum_{k=1}^N [a_k\Re(H(k\omega^*,\omega_a^*))\sin(k\omega^* t + \phi_k) + a_k\Im(H(k\omega^*,\omega_a^*))\cos(k\omega^* t + \phi_k)] + [0,0,0,0,d]^T.$$

Proof: This is an implementation of Theorem 4.1 in [37]. Note that the parameter update law (9) is approximated using averaging method:

$$\dot{\omega}_a = \frac{1}{T}\int_t^{t+T}\gamma_\omega f(y(t),\omega_a,x^0(t,\omega_a,\omega^*)) = \gamma_\omega\omega_a^2\sum_{k=1}^N a_k^2 g_k(\omega_a).$$

■

Remark 3: The robustness of ANF against the higher orders of harmonics in the input can be observed by visualizing the functions $g_k(\omega_a), k\in\{1,\dots 10\}$ using the parameters $\zeta = 0.3$, $\omega^* = \frac{2\pi}{24}$(rad/h) and $\gamma_d = 0.001$ (Figure 1). From the plot, it is clear that for the ANF with second order harmonics, $g_1(\omega_a)$ and $g_2(\omega_a)$ dominate the neighborhood of $\omega^* = \frac{pi}{12} \approx 0.2617$. The root of (12) is contributed mostly by $g_1(\omega_a)$. If the amplitudes of the higher order harmonics are small comparing with the amplitude of the fundamental harmonic, (12) has a root that satisfies (13).

The results of two simulations are plotted in Figure 2 and 3. In Figure 2, the input has ten harmonics, and the amplitude of each harmonics is 2. The waveform is severely distorted from sinusoid, but the modified ANF is still locally stable because (12) has a root and (13) is satisfied. In Figure 3, the sixth harmonic's amplitude is way too large, and (12) loses its root near ω^*, so the ANF is not locally stable near the fundamental harmonic.

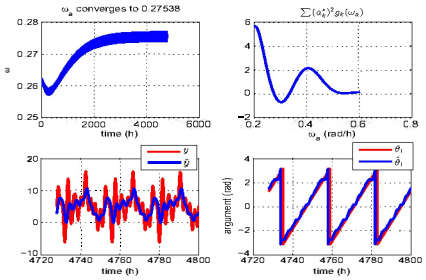

Fig. 2. a_k = [2 2 2 2 2 2 2 2 2 2] for $k \in \{1 \ldots 10\}$. $d = 5$. Upper left: in simulation, the averaged ω at the steady state is 0.275. Upper right: $\sum_{k=1}^{N} (a_k^*)^2 g_k(\omega_a) = 0$ has one root close to the fundamental harmonic: $\omega_a^* = 0.276$. Lower left: comparison of the input y and the output of the ANF $\hat{y}$. Lower right: estimated argument (wrapped to 2π).

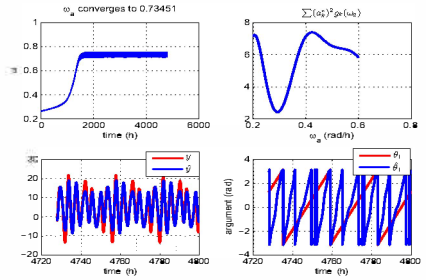

Fig. 3. a_k = [2 2 2 2 2 10 2 2 2 2] for $k \in \{1 \ldots 10\}$. $d = 5$. Upper left: in simulation, the averaged ω at the steady state is 0.75, which is not close to ω^*. Upper right: $\sum_{k=1}^{N} (a_k^*)^2 g_k(\omega_a) = 0$ has no real roots near ω^*. Lower left: comparison of the input y and the output of the ANF $\hat{y}$. Lower right: estimated argument (wrapped to 2π).

In addition to the higher order harmonics, we empirically observed the stability of the ANF under noisy input

$$y(t) = \sum_{k=1}^{N} a_k sin(k\omega^* t + \phi_k) + d + w(t).$$

where $w(t)$ is white noise with zero mean. Figure 4 shows the simulation results of the impact of white noise with large variance comparing with the amplitude of fundamental harmonic. We are currently working on rigorous analysis of the robustness of ANF against noise. In [33], we demonstrated the effectiveness of ANF on *Drosophila* and rat locomotor activity data. Using batch method as baseline, we compared the performance of ANF and gliding cosinor. For much less computation cost, ANF has similar estimation error as gliding cosinor, and much faster convergence after initialization.

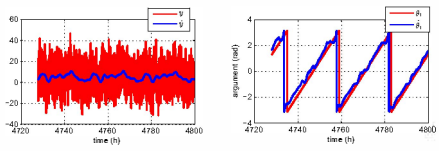

Fig. 4. a_k = [2 2 2 2 2 2 2 2 2 2] for $k \in \{1 \ldots 10\}$. $d = 5$. $Var(w) = 100$. The ANF is still tracking the fundamental harmonic.

ANF Initialization and Parameter Tuning

ANF has very good convergence property, and the state variables are easy to initialize. For circadian estimation, where the period is approximately 24 hours, ω can be initialized to be $\frac{2\pi}{24}$(rad/hr). The state variables x_1, x_2, x_3, x_4 can all be set to zero. The only parameter that needs initial guess is the constant bias x_5, which can be obtained from some sample data. For example, for human core body temperature, x_5 can be initialized at 37. The adaptation rates γ_d and γ_ω can be tuned using some sample data. The theory of integral manifold used for stability analysis is only valid for slow adaptation, so during the tuning process, the adaptation rates can be set to be very small in the beginning, and increased gradually until the performance are satisfied. ζ influences the performance of the fast dynamics. For $\zeta = 0.3$, ignoring the much slower dynamics of parameters adaptation, the convergence rate is approximately $e^{\frac{-t}{0.1\text{hr}}}$.

III. Circadian Control Based on ANF

There are multiple attractive features of the proposed circadian argument estimator: it does not require the knowledge of a highly complex nonlinear model; it can handle parameters' change and noisy signal, and has well defined tunable parameters for the trade-off between convergence rate and noise rejection.

The ANF extracts the circadian argument from past measurements, and it lacks predictive capability to the evolution of the circadian rhythm under different light inputs because there is no structure of the underlying mechanism linking light input to the measurements. However, if we combine the circadian system with the ANF as the plant, the model of the combination can be identified using the light input and ANF's argument estimation. The overall architecture of the closed loop system is shown in Figure 5. The major advantage of this method is that we do not need to know the underlying circadian dynamics model, which is complex and usually not available; all we need are the lighting that can stimulate the circadian rhythm, and continuously measured circadian data which can serve as a circadian marker. In this paper, the proposed method is evaluated using three existing circadian models: Kronauer' human circadian model [34], Leloup's 10-state *Drosophila* biochemical model and Leloup's 3-state *Neurospora* biochemical model [35].

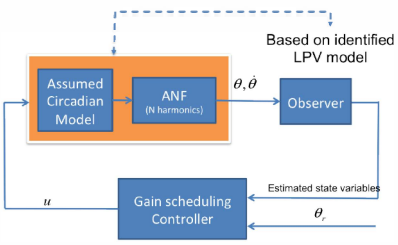

Fig. 5. Architecture of preliminary control investigation. Three assumed models have been used: the 2-state empirical nonlinear oscillator model by Kronauer, the 10-state drosophila gene network model, and the 3-state neurospora gene network model.

A. Linear Parameter Varying Model Identification

All three circadian models can be expressed in the following form:

$$\dot{z} = f(z,u) \tag{14}$$

where z is the vector of state variables, and u is the bounded control input related with lighting. In darkness, every model has a stable limit cycle with period τ.

Assume that we do not know the circadian dynamics model(14). We can only control the input u by tuning the light and continuously measure some physiological output $y = h(z)$ as the circadian data. For the three circadian models, we make the following assumptions about the measurable physiological output:

- For the simplified Kronauer's human model, y is the core body temperature (CBT) which can be approximated as $y = 37 + [1,0]z$.
- For the *Drosophila* model, $y = [0,1,1,1,0,0,0,0,1,1]z$ is the total concentration of protein *PER*.
- For the *Neurospora* model, $y = [0,1,1]z$ is the concentration of the protein *FRQ*.

y is the input of the ANF which estimates both $\hat{\theta}$ and $\dot{\hat{\theta}}$. If $\hat{\theta}(t)$ is used for modeling, the identified system would be unstable since the argument increases in magnitude with time. We therefore choose $\dot{\hat{\theta}}$ as the model output (which may be directly obtained from (11) without numerical differentiation). In this case the identified system is stable.

We identify the system using a batch of impulse response curves. 10-min light pulses are applied at phase argument θ_{pulse}, and the impulse response $\dot{\hat{\theta}}$ is fit to a second order discrete time LTI model suing subspace identification:

$$x_{k+1} = A(\theta_{pulse})x_k + B(\theta_{pulse})u_k \tag{15}$$

$$\dot{\hat{\theta}}_k = C(\theta_{pulse})x_k + \dot{\hat{\theta}}_{free\ running} \tag{16}$$

where $\dot{\hat{\theta}}_{free\ running} = \frac{2\pi}{\tau}$. For different θ_{pulse}, we obtain a batch of LTI models. In observer canonical form, all these LTI models have the same $C(\theta_{pulse})$ and similar $A(\theta_{pulse})$, but $B(\theta_{pulse})$ matrices are varying with θ_{pulse}. Combine the LTI models into a LPV model with the following form

$$x_{k+1} = Ax_k + B(\hat{\theta})u_k \tag{17}$$

$$\dot{\hat{\theta}}_k = Cx_k + \dot{\hat{\theta}}_{free\ running} \tag{18}$$

where A is the average of $A(\theta_{pulse})$, $C = [0,1]$ and $B(\hat{\theta})$ is a function of the estimated circadian argument $\hat{\theta}$ during the light pulse.

To validate the LPV model, we apply multiple light pulses with random timing and random duration to the Kronauer's model, the *Drosophila* model and the *Neurospora* model. The results show that LPV model identification has good predictive capability on $\dot{\hat{\theta}}$ (Figure 6).

B. Light Based Circadian Phase Control

Once the LPV model is obtained, we can use the model to design light input to achieve the desired objective. This problem has typically been posed as a phase shift control problem

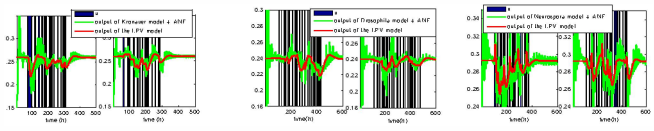

(a) Human model (b) *Drosophila* (c) *Neurospora*

Fig. 6. The LPV model identified by using the output of the Kronauer model and the LeLoup models cascaded with the ANF

and the phase response curve has commonly been used as the basis for circadian rhythm control [3], [4], [6], [17], [34], [38]. Since PRC is a steady state characterization, there is no transient regulation. One can achieve the required phase shift asymptotically, but there is no guarantee on how fast that could be attained. Furthermore, there is no disturbance rejection during the transient. Our preliminary approach is to use a gain scheduling controller to let $\hat{\theta}(t)$ track a reference argument $\theta_r(t)$, which is increasing with the rate $\dot{\theta}_r = \frac{2\pi}{\tau}$. We design an output feedback controller for each LTI model in the LPV model description. These LTI controllers are then combined together through interpolation using the estimated argument $\hat{\theta}(t)$ (essentially a gain scheduling controller). The control input u is bounded.The closed loop circadian argument regulation results for the three cases are plotted in Figure 7. With some controller tuning, the system exhibits asymptotic stability when the desired circadian argument θ_r is shifted to simulate the situation of the jet lag.

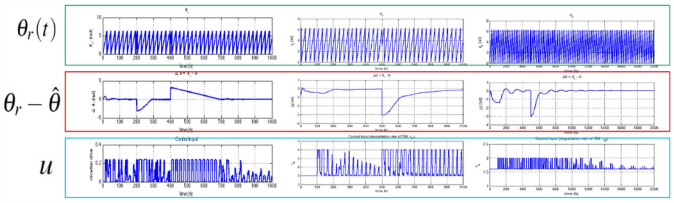

Fig. 7. Preliminary result on LPV-based lighting control with the Kronauer model (left), the Leloup *Drosophila* model (middle), and the Leloup *Neurospora* model (right) as the circadian rhythm truth model. The reference circadian argument θ_r is commanded with π phase shift to simulate the jet lag recovery. Using the LPV approximation and ANF circadian argument estimate, the gain scheduling controller reduces the argument tracking error to zero.

IV. Conclusion and Future Work

This paper presents an adaptive circadian argument estimator which extracts the argument of the fundamental harmonic in the circadian data. The estimator is based on adaptive notch filter. The local stability is analyzed. Taking advantage of the proposed circadian estimator, a modeling and control method based on LPV is presented. The major advantage of this method is that the biological system can be considered as a black box, and no model of the circadian dynamics is required. The controlled plant is the combination of the biological system and the estimator. The input of the plant is light, and the output is circadian argument estimation. The LPV model of the plant is identified using a batch

method, and gain scheduling is used to regulate the estimated circadian argument to the desired circadian argument. The proposed modeling and control method is applied to the human circadian model, the *Drosophila* circadian model and the *Neurospora* circadian model. In all the three cases, the circadian arguments can be stabilized. In the future, we will work on the *Drosophila* experiment demonstration of the proposed circadian estimation/control strategy, and develop a recursive identification method of the LPV model.

ACKNOWLEDGMENT

This work was supported in part by the National Science Foundation (NSF) Smart Lighting Engineering Research Center (EEC-0812056), and in part by the Center for Automation Technologies and Systems (CATS) under a block grant from the New York State Empire State Development Division of Science, Technology and Innovation (NYSTAR). The authors would also like to thank Mariana Figueiro, Mark Rea, and Andrew Bierman for introducing the authors to the circadian rhythm research and many helpful discussions.

REFERENCES

[1] M.E. Jewett, R.E. Kronauer, and C.A. Czeisler. Phase-amplitude resetting of the human circadian pacemaker via bright light: A further analysis. *Journal of Biological Rhythms*, 9:295–314, 1994.

[2] M.E. Jewett, D.W. Rimmer, J.F. Duffy, E.B. Klerman, R.E. Kronauer, and C.A. Czeisler. Human circadian pacemaker is sensitive to light throughout subjective day without evidence of transients. *American Journal of Physiology – Regulatory, Integrative and Comparative Physiology*, 273:1800–1809, 1997.

[3] C. Mott, D. Mollicone, M. Van Wollen, and M. Huzmezan. Modifying the human circadian pacemaker using model based predictive control. In *2003 American Control Conference*, pages 453–458, Denver, CO, 2003.

[4] N. Bagheri, J. Stelling, and F.J. Doyle III. Optimal phase-tracking of the nonlinear circadian oscillator. In *2005 American Control Conference*, pages 3235–3240, Portland, OR, 2005.

[5] C. Gronfier, Jr. K.P. Wright, R.E. Kronauer, and C.A. Czeisler. Entrainment of the human circadian pacemaker to longer-than-24-h days. *Proceedings of National Academy of Science*, 104(21):9081–9086, 2007.

[6] D.A. Dean II, D.B. Forger, and E.B. Klerman. Taking the lag out of jet lag through model based schedule design. *PLoS Computational Biology*, 5(6), June 2009.

[7] J. Zhang, A. Bierman, J.T. Wen, A. Julius, and M.G. Figueiro. Circadian system modeling and phase control. In *Conference on Decision and Control*, Atlanta, GA, 2010.

[8] J. Zhang, J.T. Wen, and A. Julius. Optimal circadian rhythm control with light input for rapid entrainment and improved vigilance. In *Conference on Decision and Control*, Maui, HI, 2012.

[9] A.J. Lewy, S. Ahmed, J.L. Jackson, and R.L. Sack. Melatonin shifts human orcadian rhythms according to a phase-response curve. *Chronobiology international*, 9(5):380–392, 1992.

[10] M. Harrington. Location, location, location: important for jet-lagged circadian loops. *Journal of Clinical Investigation*, 120(7):2265–2267, July 2010.

[11] M. Jakovljević. Agomelatine as chronopsychopharmaceutics restoring circadian rhythms and enhancing resilience to stress: a wishfull thinking or an innovative strategy for superior management of depression? *Psychiatria Danubina*, 23(1):2–9, 2011.

[12] D.S. Minors, J.M. Waterhouse, and A. Wirz-Justice. A human phase-response curve to light. *Neuroscience letters*, 133(1):36–40, 1991.

[13] E. De Maria, F. Fages, and S. Soliman. On coupling models using model-checking: Effects of irinotecan injections on the mammalian cell cycle. In *CMSB'09: Seventh International Conference on Computational Methods in Systems Biology*, pages 142–157, 2009.

[14] E. De Maria, F. Fages, A. Rizk, and S. Soliman. Design, optimization and predictions of a coupled model of the cell cycle, circadian clock, dna repair system, irinotecan metabolism and exposure control under temporal logic constraints. pre-print submitted to Theoretical Computer Science, 2011.

[15] Philips. Product manual of HF3332 and HF3331. www.lighttherapy.philips.com.

[16] M. Terman and J.S. Terman. Light therapy for seasonal and non-seasonal depression: efficacy, protocol, safety and side effects. *CNS Spectrum*, 10(8):647, 2005.

[17] N. Bagheri, J.Stelling, and F.J. Doyle III. Circadian phase entrainment via nonlinear model predictive control. *Int. J. of Robust & Nonlinear Control*, 17:1555–1571, 2007.

[18] K.D. Frank and W.F. Zimmerman. Action spectra for phase shifts of a circadian rhythm in drosophila. *Science*, 163(3868):688–689, 1969.

[19] S. Daan and C.S. Pittendrigh. A functional analysis of circadian pacemakers in nocturnal rodents. II. the variability of phase response curves. *Journal on Computational Physiology*, 106:253266, 1976.

[20] G.C. Brainard, J.P. Hanifin, J.M. Greeson, B. Byrne, G. Glickman, E. Gerner, and M.D. Rollag. Action spectrum for melatonin regulation in humans: evidence for a novel circadian photoreceptor. *Journal of Neuroscience*, 21(16):6405–6412, 2001.

[21] A. Klarsfeld, J.C. Leloup, and F. Rouyer. Circadian rhythms of locomotor activity in drosophila. *Behavioural Processes*, 64:161–175, 2003.

[22] S. Ancoli-Israel, R. Cole, C. Alessi, M. Chambers, W. Moorcroft, and C. Pollak. The role of actigraphy in the study of sleep and circadian rhythms. american academy of sleep medicine review paper. *Sleep*, 26(3):342–92, 2003.

[23] J. Zhang, J.T. Wen, A.Julius, A. Bierman, and M.G. Figueiro. Modeling of drosophila circadian system based on the locomotor activity. In *2011 American Control Conference*, San Francisco, CA, June 2011.

[24] R. Refinetti, G. Cornelissen, and F. Halberg. Procedures for numerical analysis of circadian rhythms. *Biological Rhythm Research*, 38:275–325, 2007.

[25] R. Refinetti. *Circadian physiology*. CRC Press, 2006.

[26] J. T. Enright. The search for rhythmicity in biological time series. *Journal of Theoretical Biology*, 8:426–468, 1965.

[27] M. H. Teicher and N. I. Barber. Cosifit: An interactive program for simultaneous multioscillator cosinor analysis of time-series data. *Computers and Biomedical Research*, 23:283–295, 1990.

[28] E. Batschelet. *Circular Statistics in Biology.* Academic Press., New York, 1981.

[29] P. Indic and E.N. Brown. Characterizing the amplitude dynamics of the human core-temperature circadian rhythm using a stochastic–dynamic model. *Journal of Theoretical Biology*, 239(4):499–506, 2006.

[30] C. Mott, G. Dumont, D. B. Boivin, and D. Mollicone. Model-based human circadian phase estimation using a particle filter. *IEEE Transactions on Biomedical Engineering*, 58(5):1325–1336, 2011.

[31] S. Nintcheu-Fata, G. Cornlissen, G. Katinas, F. Halberg, B. Fier, J. Siegelov, M. Maek, and J. Duek. Software for contour maps of moving least-squares spectra. *Scripta medica*, 76:279–283, 2003.

[32] L. Hsu, R. Ortega, and G. Damm. A Globally Convergent Frequency Estimator. *IEEE Transaction on Automatic Control*, 44(4):698–713, 1999.

[33] J. Zhang, J.T. Wen, and A. Julius. Adaptive circadian rhythm estimator and its application to locomotor activity. In *IEEE Signal Processing in Medicine and Biology Symposium*, New York, NY, December 2012.

[34] R.E. Kronauer, D.B. Forger, and M.E. Jewett. Quantifying human circadian pacemaker response to brief, extended, and repeated light stimuli over the phototopic range. *Journal of Biological Rhythms*, 14(6):501–516, 1999.

[35] J.C. Leloup, D. Gonze, and A. Goldbeter. Limit cycle models for circadian rhythms based on transcriptional regulation in drosophila and neurospora. *Journal of Biological Rhythms*, 14(6):433–448, 1999.

[36] P. Tichavsky and A. Nehorai. Comparative study of four adaptive frequency trackers. *IEEE Transaction on Signal Processing*, 45(6):1473–1484, 1997.

[37] B. Riedle and P. Kokotovic. Integral manifolds of slow adaptation. *IEEE Transactions on Automatic Control*, 31(4):316–324, 1986.

[38] F.J. Doyle III, R. Gunawan, N. Bagheri, H. Mirsky, and T.L. To. Circadian rhythm: A natural, robust, multi-scale control system. *Computers & Chemical Engineering*, 30(10-12):1700–1711, 2006.